A Mathematical Tutorial on Synthetic Aperture Radar

Margaret Cheney
Department of Mathematical Sciences
Rensselaer Polytechnic Institute
chenem@rpi.edu

February 9, 2001

Abstract

This paper presents the foundations of conventional strip-mode Synthetic Aperture Radar from a mathematical point of view. In particular, the paper shows how a simple antenna model can be used together with a linearized scattering approximation to predict the received signal. The conventional matched-filter processing is explained and analyzed to exhibit the resolution of the SAR system.

1 Introduction and Background

In conventional strip-mode Synthetic Aperture Radar (SAR) imaging, a plane or satellite flies along a straight track, which we will assume is in the direction of the x_2 axis. The antenna emits pulses of electromagnetic radiation in a directed beam perpendicular to the flight track (i.e., in the x_1 direction). These waves scatter off the terrain, and the scattered waves are detected with the same antenna. The received signals are then used to produce an image of the terrain. (See Figure 1.)

The data depend on two variables, namely time and position along the x_2 axis, so we expect to be able to reconstruct a function of two variables.

The correct model for radar is of course Maxwell's equations, but the simpler scalar wave equation is commonly used:

$$\left(\nabla^2 - \frac{1}{c^2(x)}\partial_t^2\right) U(t, x) = 0. \tag{1}$$
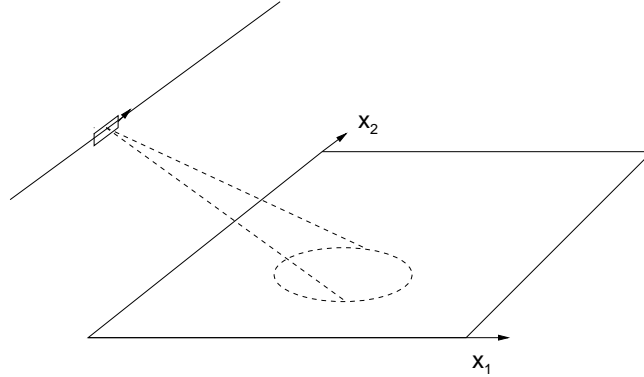
Figure 1: This shows the geometry of a SAR system.

This is the equation satisfied by each component of the electric and magnetic fields in free space, and is thus a good model for the wave propagation in dry air. When the electromagnetic waves interact with the ground, their polarization is certainly affected, but if the SAR system does not measure this polarization, then (1) is an adequate model.

We assume that the earth is roughly situated at the plane $x_3 = 0$, and that for $x_3 > 0$, the wave speed is $c(x) = c_0$, the speed of light in vacuum (a good approximation for dry air).

In free space, the field $G_0(t - \tau, x - y)$ at x, t due to a delta function point source at position y and time τ is given by [16]

$$G_0(t - \tau, x - y) = \frac{\delta(t - \tau - |x - y|/c_0)}{4\pi |x - y|}. \tag{2}$$

This field satisfies the equation

$$\left(\nabla^2 - \frac{1}{c_0^2} \partial_t^2 \right) G_0(t - \tau, x - y) = -\delta(t - \tau)\delta(x - y). \tag{3}$$

2   The incident wave

We assume that the signal sent to the antenna is

$$P(t) = A(t)e^{i\omega_0 t}, \tag{4}$$

where the frequency $\omega_0/2\pi$ is called the *carrier frequency* and A is a slowly varying amplitude that is allowed to be complex.

If the source at y has the time history (4), then the resulting field $U_y(t, z - y)$ satisfies the equation

$$\left(\nabla^2 - \frac{1}{c_0^2} \partial_t^2 \right) U_y(t, z - y) = -P(t)\delta(z - y) \tag{5}$$

2

and is thus given by

$$
\begin{aligned}
U_y(t, z) = (G_0 * P)(t, z - y) &= \int \frac{\delta(t - \tau - |z - y|/c_0)}{4\pi|z - y|} P(\tau) d\tau \\
&= \frac{P(t - |z - y|/c_0)}{4\pi|z - y|} \\
&= \frac{A(t - |z - y|/c_0)}{4\pi|z - y|} e^{i\omega_0(t - |z - y|/c_0)}.
\end{aligned} \tag{6}
$$

The antenna, however, is not a point source. Most conventional SAR antennas are either slotted waveguides [6, 18, 10] or microstrip antennas [15], and in either case, a good mathematical model is a rectangular distribution of point sources. We denote the length and width of the antenna by L and D, respectively. We denote the center of the antenna by x; thus a point on the antenna can be written $y = x + q$, where q is a vector from the center of the antenna to a point on the antenna. We also introduce coordinates on the antenna: $q = s_1\hat{e}_1 + s_2\hat{e}_2$, where $\hat{e}_1$ and $\hat{e}_2$ are unit vectors along the width and length of the antenna, respectively. The vector $\hat{e}_2$ points along direction of flight; for the straight flight track shown in Figure 1, this would be the x_2 axis. For side-looking systems as shown in Figure 1, $\hat{e}_1$ is tilted with respect to the x_1 axis so that a vector perpendicular to the antenna points to the side of the flight track.

We consider points z that are far from the antenna; for such points, for which $|q| << |z - x|$, we have the approximation

$$
|z - y| = |z - x| - (\widehat{z - x}) \cdot q + O(L^2/|z - x|), \tag{7}
$$

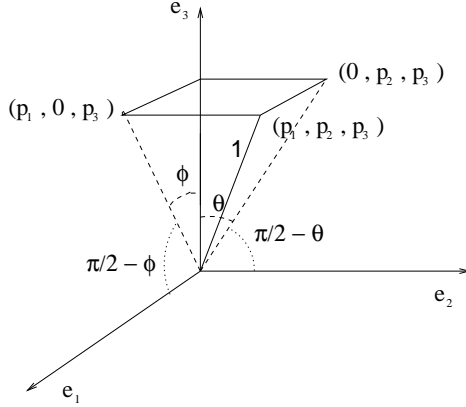where the hat denotes a unit vector. We use this expansion in (6):

$$
U_y(t, z) \sim \frac{A(t - |z - x|/c_0 + \widehat{z - x} \cdot q/c_0 + \cdots)}{4\pi|z - x|} e^{i\omega_0(t - |z - x|/c_0)} e^{ik\widehat{z - x} \cdot q} \tag{8}
$$

where we have written $k = \omega_0/c_0$. This expansion is valid because we also have $kL^2 << |z - x|$. We now make use of the fact that $|z - x| >> \widehat{z - x} \cdot q$ and that A is assumed to be slowly varying to write

$$
U_y(t, z) \sim \frac{P(t - |z - x|/c_0)}{4\pi|z - x|} e^{ik\widehat{z - x} \cdot q}. \tag{9}
$$

Far from the antenna, the field from the antenna is

$$
\begin{aligned}
U_x^{in}(t, z) &= \int_{-L/2}^{L/2} \int_{-D/2}^{D/2} U_{x + s_1\hat{e}_1 + s_2\hat{e}_2}(t, z) ds_1 ds_2 \\
&\sim \int_{-L/2}^{L/2} \int_{-D/2}^{D/2} \frac{P(t - |z - x|/c_0)}{4\pi|z - x|} e^{ik\widehat{z - x} \cdot (s_1\hat{e}_1 + s_2\hat{e}_2)} ds_1 ds_2
\end{aligned}
$$

3

e_3

$(0, p_2, p_3)$

$(p_1, 0, p_3)$

(p_1, p_2, p_3)

1

ϕ

θ

$\pi/2 - \theta$

$\pi/2 - \phi$

e_2

e_1

Figure 2: This is a diagram that shows that if $p = \widehat{z - x}$ is a unit vector, then $\hat{p} \cdot \hat{e}_2 = p_2 \approx \sin\theta$ and $\hat{p} \cdot \hat{e}_1 = p_1 \approx \sin\phi$. Here θ is the angle between the vector normal to the antenna and the projection of $\widehat{z - x}$ on the e_1-e_3 plane. In this figure, the antenna lies on the e_1-e_2 plane.

$$\sim \quad \frac{P(t - |z - x|/c_0)}{4\pi|z - x|} \int_{-D/2}^{D/2} e^{iks_1 \widehat{z-x} \cdot \hat{e}_1} ds_1 \int_{-L/2}^{L/2} e^{iks_2 \widehat{z-x} \cdot \hat{e}_2} ds_2$$
$$\sim \quad \frac{P(t - |z - x|/c_0)}{4\pi|z - x|} w(\widehat{z - x}),$$

$$(10)$$

where

$$w(\widehat{z - x}) = 2D\mathrm{sinc}(k\widehat{z - x} \cdot e_1 D/2) \, 2L\mathrm{sinc}(k\widehat{z - x} \cdot e_2 L/2) \qquad (11)$$

is the antenna beam pattern and where $\mathrm{sinc}\,\beta = (\sin\beta)/\beta$. The sinc function has its main peak at $\beta = 0$ and its first zero at $\beta = \pi$; this value of β gives half the width of the main peak. Thus the main beam of the antenna is directed perpendicular to the antenna. The first zero of $\mathrm{sinc}(k\widehat{z - x} \cdot e_2 L/2)$ occurs when $k\widehat{z - x} \cdot \hat{e}_2 L/2 = \pi$. Using the fact that $2\pi/k$ is precisely the wavelength λ, we can write this as $\widehat{z - x} \cdot \hat{e}_2 = \lambda/L$. To understand this condition, we write $\widehat{z - x} \cdot \hat{e}_2 \approx \cos(\pi/2 - \theta) = \sin\theta \approx \theta$, an approximation that is valid for small angles θ. (See Figure 2.) Thus when $\lambda << L$ and thus θ is small, the condition $\widehat{z - x} \cdot \hat{e}_2 = \lambda/L$ reduces to $\theta \approx \lambda/L$. In this case, the main lobe of the antenna beam pattern has angular width $2\lambda/L$ in the $\hat{e}_2$ direction. Similarly the angular width in the $\hat{e}_1$ direction is $2\lambda/D$. We note that smaller wavelengths and larger antennas correspond to more tightly focused beams.

4

3 A linearized scattering model

From classical scattering theory we know that a scattering solution of (1) can be written

$$\Psi(t, x) = \Psi^{in}(t, x) + \Psi^{sc}(t, x), \tag{12}$$

where Ψ^{in} satisfies (1) with $c(x) = c_0$ and where (see Appendix)

$$\Psi^{sc}(t, x) = \int\int G_0(t - \tau, x - z)V(z)\partial_\tau^2 \Psi(\tau, z)d\tau d^3 z \tag{13}$$

and

$$V(z) = \frac{1}{c_0^2} - \frac{1}{c^2(z)}. \tag{14}$$

For commonly used carrier frequencies ω_0, the waves decay rapidly as they penetrate into the earth. Thus the support of V can be taken to be a thin layer at the earth's surface. Thus we assume that V is of the form $V(z) = V(z_1, z_2)\delta(z_3)$.

A commonly used approximation, called the *Born approximation* or the *single scattering approximation*, is to replace Ψ on the right side of (13) by the incident field Ψ^{in}:

$$
\begin{aligned}
\Psi^{sc}(t, x) \approx \Psi^B(t, x) &= \int\int G_0(t - \tau, x - z)V(z)\partial_\tau^2 \Psi^{in}(t, x)d\tau d^3 z \\
&= \int \frac{V(z)}{4\pi|x - z|}\partial_t^2 \Psi^{in}(t - |x - z|/c_0, z)d^3 z. \quad (15)
\end{aligned}
$$

The value of this approximation is that it removes the nonlinearity in the inverse problem: it replaces the product of two unknowns (V and Ψ) by a single unknown (V) multiplied by the known incident field.

Another linearizing approximation that can be used at this point is the *Kirchhoff approximation*, in which the scattered field is replaced by its geometrical optics approximation [12]. Here, however, we consider only the Born approximation.

In the case of SAR, the antenna emits a series of fields of the form (10) as it moves along the flight track. In particular, we assume that the antenna is located at position x^n at time nT, and there emits a field of the form (10). In other words, the incident field is

$$\Psi^{in}(\tau, z) = \sum_n \Psi_n^{in}(\tau, z), \tag{16}$$

where

$$
\begin{aligned}
\Psi_n^{in}(\tau, z) = U_{x^n}^{in}(\tau - nT, z) &= \int\int_{\text{antenna}} U_{x^n + q}(\tau - nT, z)d^2 q \\
&\sim \frac{P(\tau - nT - |z - x^n|/c_0)}{4\pi|z - x^n|}w(\widehat{z - x^n}) \quad (17)
\end{aligned}
$$

is the nth emission. We use this expression in (15) to find an approximation to the scattered field due to the nth emission. The resulting expression involves two time derivatives of $P(t, x)$. In calculating these time derivatives, we use the fact that A is assumed to be slowly varying to obtain

$$\partial_t^2 P(t, x) \approx -\omega_0^2 P(t, x). \tag{18}$$

Thus the Born approximation to the scattered field due to the nth emission, measured at the center of the antenna, is

$$
\begin{aligned}
S_n(t) &\approx \Psi_n^B(t - nT, x^n) \\
&\approx -\int \frac{\omega_0^2 P(t - nT - 2|z - x^n|/c_0)}{4\pi|z - x^n|} \frac{V(z)}{4\pi|z - x^n|} w(z \widehat{- x^n}) d^3z.
\end{aligned} \tag{19}
$$

In (19), we note that $2|z - x^n|/c_0$ is the two-way travel time from the center of the antenna to the point z. The factors $4\pi|z - x^n|$ in the denominator correspond to the geometrical spreading of the spherical wave emanating from the antenna and from the point z.

In practice, the received signal is not measured at a single point in the center of the antenna; rather, the signal is received on the entire antenna. This means that the received signal is subject to the same weighting as the transmitted signal. Thus w in (19) should be replaced by w^2. We continue to write simply w.

In (19), we approximate the factors of $|z - x^n|$ in the denominator by R_0, the distance from z to the flight track (see Figure 3), an approximation which is justified because $|z - x^n|^{-1}$ is a slowly varying function of n.

4 Matched filter processing

To form an image, first a *matched filter* is applied to the received signal $S_n(t)$:

$$I_n(y) = \int \overline{P(t - nT - 2|y - x^n|/c_0)} S_n(t) dt, \tag{20}$$

where the bar denotes complex conjugate. This is called a matched filter because one "matches" the received signal against a signal proportional to that due to a "point scatterer" at position y (i.e., take $V(z) = \delta(z - y)$ in the Born approximation). A matched filter is used because it is the optimal linear filter in the sense of providing the best signal-to-noise ratio [3].

If we use expression (19) (with $|z - x^n|$ replaced by R_0) in (20) and interchange the order of integration, we find

$$I_n(y) \approx \int W_n(y, z) \frac{-\omega_0^2 V(z)}{(4\pi R_0)^2} dz, \tag{21}$$

where

$$W_n(y, z) = w(z \widehat{\,-\,} x^n) \int \overline{P(t - nT - 2|y - x^n|/c_0)} P(t - nT - 2|z - x^n|/c_0) dt \tag{22}$$

represents the *point spread function* of this single-look imaging system: if $V(z) = \delta(z - z_0)$, then $I_n(y) = W_n(y, z_0)$ would be proportional to the resulting image of V. Our goal is to make this point spread function as close to a delta function as possible. The key idea of SAR is that this point spread function can be improved by summing over n, i.e., by combining information from multiple looks. We thus consider

$$I(y) = \sum_n I_n(y) \approx \int W(y, z) \frac{-\omega_0^2 V(z)}{(4\pi R_0)^2} dz, \tag{23}$$

with the point spread function

$$W(y, z) = \sum_n W_n(y, z) \tag{24}$$

This point spread function is called the *generalized ambiguity function* of the SAR system. We want to choose P so as to make W as close to a delta function as possible.

5 Resolution

Resolution of the system can be determined by an investigation of the generalized ambiguity function (24). Under the assumption (4) we write W as

$$W(y, z) = \sum_n w(z \widehat{\,-\,} x^n) \int \overline{A(t - nT - 2|y - x^n|/c_0)} e^{-i\omega_0(t - nT - 2|y - x^n|/c_0)} \\ A(t - nT - 2|z - x^n|/c_0) e^{i\omega_0(t - nT - 2|z - x^n|/c_0)} dt. \tag{25}$$

In (25), we make the change of variables $t - nT \to t$, and then use the fact that A is slowly varying. In this approximation, the As no longer depend on n and can be pulled out of the sum. The time dependence in the exponentials cancels out, and thus the ambiguity function factors as
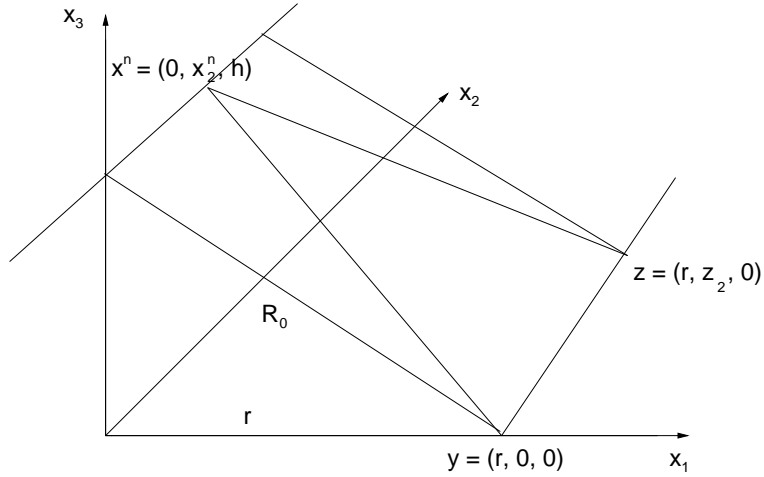
$$W(y, z) \approx W_R(y, z) W_A(y, z), \tag{26}$$

where
$$W_R(y, z) = \int \overline{A(t - 2|y - x^n|/c_0)} A(t - 2|z - x^n|/c_0) dt \tag{27}$$

and
$$W_A(y, z) = \sum_n e^{i2k(|y - x^n| - |z - x^n|)} w(z \widehat{\,-\,} x^n), \tag{28}$$

Figure 3: This shows the geometry for computation of the azimuthal resolution.

where $k = \omega_0/c_0$. The first factor of (26), W_R, expressed in the "fast time" t by (27), controls the range resolution. The second factor of (26), W_A, is expressed via (28) in terms of the position variable x^n, which is sometimes called "slow time" because it corresponds to the relatively slow movement along the flight track. The factor W_A controls the azimuthal ("Doppler") resolution.

5.1 Azimuthal resolution

To study the azimuthal resolution, we consider two points y and z at the same range, i.e., at the same distance R_0 from the flight track. In particular, we write $y = (r, 0, 0)$ and $z = (r, z_2, 0)$. We assume that the range R_0 is much greater than the distances along the flight path, so that $|x_2^n| << R_0$ and $|x_2^n - z_2| << R_0$. (See Figure 3.)

We use the Pythagorean theorem, factor out R_0, and then expand the remaining square roots to obtain large-R_0 asymptotic expansions for the distances appearing in (28):

$$
\begin{aligned}
|x^n - y| &= \sqrt{R_0^2 + (x_2^n)^2} = R_0\sqrt{1 + (x_s^n/R_0)^2} \approx R_0 + \frac{(x_2^n)^2}{2R_0} + \cdots \\
|x^n - z| &= \sqrt{R_0^2 + (x_2^n - z_2)^2} \approx R_0 + \frac{(x_2^n - z_2)^2}{2R_0} + \cdots
\end{aligned}
\tag{29}
$$

We use these expansions in the exponentials of (28). When we do this, the two terms that come from $|x^n - y|$ cancel, and we are left with

$$
W_A(y, z) \sim \sum_n e^{ik(2x_2^n z_2 - z_2^2)/R_0} w(z \widehat{-} x^n).
\tag{30}
$$

8

The second term in the exponent is independent of n and can be taken outside the sum. In the first term, we use the fact that $x_2^n = nvT$, where v is the speed with which the antenna moves along the flight track. Thus (30) can be written

$$W_A(y, z) \sim e^{-ikz_2^2/R_0} \sum_n \left(e^{2ikz_2vT/R_0}\right)^n w(\widehat{z - x^n}). \tag{31}$$

The range of n values in this sum is effectively determined by the width of the antenna beam pattern w (11). To determine the limits, we approximate the relevant sinc function by a characteristic function whose width is the same as that of the main lobe of the sinc: $\mathrm{sinc}\beta \approx \chi_{[-\pi,\pi]}(\beta)$, where $\chi_{[-\pi,\pi]}$ denotes the function that is one in the interval $[-\pi, \pi]$ and zero outside. By doing this, we find that w is effectively nonzero only when

$$-\pi < \frac{kL}{2} \frac{(z_2 - x_2^n)}{|z - x^n|} < \pi. \tag{32}$$

In (32) we use the large-R_0 approximation (29) and then solve for x_2^n:

$$z_2 - \lambda R_0/L < x_2^n < z_2 + \lambda R_0/L, \tag{33}$$

where we have used the fact that $\lambda = 2\pi/k$. We see from (33) that the antenna moves a distance of

$$L_{\mathrm{eff}} = 2\lambda R_0/L \tag{34}$$

while the point z remains in the beam. This is thus the effective length of the synthetic array. It is the same as the width of the footprint, at range R_0, due to an antenna with angular beamwidth $2\lambda/L$.

When we use $x_2^n = nvT$ in (33) and solve for n, we find that

$$\frac{1}{vT}\left(z_2 - \frac{\lambda R_0}{L}\right) < n < \frac{1}{vT}\left(z_2 + \frac{\lambda R_0}{L}\right). \tag{35}$$

Using this in (31), we find that

$$W_A(y, z) \sim e^{ikz_2^2/R_0} 4LD\mathrm{sinc}((kD/2)\sin\phi) \sum_{n=-N/2}^{N/2} \left(e^{2ikz_2vT/R_0}\right)^n, \tag{36}$$

where N is the greatest integer less than $2\lambda R_0/(vTL)$ and $\widehat{z - x^n} \cdot \hat{e}_1 \approx \sin\phi$. The sum of exponentials in (36) is calculated in the appendix. We obtain

$$W_A(y, z) \sim e^{ikz_2^2/R_0} 4LD\mathrm{sinc}((kD/2)\sin\phi)\frac{\sin(kz_2vT(N+1)/R_0)}{\sin(kz_2vT/R_0)}. \tag{37}$$

The argument of the sine function in the denominator of (37) is small, so the denominator is approximately kz_2vT/R_0. The argument in the numerator, on the

other hand, involves the synthetic array length $vT(N+1) \approx vT2\lambda R_0/(vTL) = 2\lambda R_0/L = L_{\text{eff}}$. Thus (37) is approximately

$$W_A(y, z) \approx e^{ikz_2^2/R_0} 4LD \text{sinc}((kD/2)\sin\phi)\frac{\sin(kz_2 L_{\text{eff}}/R_0)}{kz_2 vT/R_0}. \tag{38}$$

The exponential in (38) has modulus one; the remaining factor is proportional to a sinc function with argument involving z_2. The azimuthal resolution is therefore determined by the value of z_2 for which the argument of the sine function is equal to π, namely

$$z_2 = \frac{\pi R_0}{k L_{\text{eff}}} = \frac{\lambda R_0}{2 L_{\text{eff}}}. \tag{39}$$

This is half the width of the main lobe. The full width is thus

$$2z_2 = \frac{\lambda R_0}{L_{\text{eff}}} = L/2, \tag{40}$$

where we have used (34).

Expression (40) is the azimuthal resolution of the SAR system. It is a very surprising result, for 3 reasons: 1) it is independent of range; 2) it is independent of λ; and 3) it is better for small antennas. The explanation for all three of these features lies in the effective length of the synthetic array. When a scatterer is farther away, it stays in the beam longer, so for such a point, the effective length of the synthetic array is greater. Longer wavelengths and smaller antennas give rise to broader antenna beam patterns, so that again, the synthetic array is effectively larger.

5.2   Range resolution

At this point, our only assumption about P has been (4). Thus we still have freedom to choose A to improve the range resolution.

Consider the problem of resolving of two point scatterers whose positions differ by a range Δr. To get perfect resolution, we would like to use a delta function pulse; then the time separation of the return pulses would be $\Delta t = 2\Delta r/c_0$. A system in which the time sampling is finer than this would be able to determine that the two scatterers were located at different ranges.

Unfortunately, it is not practical to transmit an infinite-energy pulse such as a delta function. If one uses instead a wave that is zero outside a time window of length τ, then the return waves don't overlap if $\tau < 2\Delta r \ c_0$. Thus a wavetrain of length τ can resolve two scatterers if their ranges Δr differ by $\Delta r > \tau c_0/2$. Thus, to get good resolution, we would like to use a very short wavetrain.

10
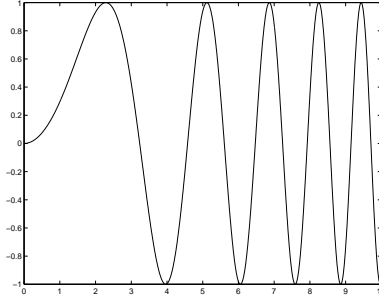
Figure 4: The chirp $\sin(.3t^2)$.

Unfortunately, because any transmitted field is necessarily limited in amplitude, short wavetrains also have very low energy. This means that little energy is reflected from the target, and these low-energy scattered waves will get drowned out by noise. Thus short pulses cannot be used.

To circumvent this difficulty, SAR systems use *pulse modulation*, in which one transmits a complex waveform and then *compresses* the received signal, generally by matched filter processing, to synthesize the response from a short pulse. The most commonly used modulated pulse is a *chirp*, which involves linear frequency modulation. The idea is to label different parts of the wave by their frequency, and then superimpose these different parts in the compression process.

5.2.1   Instantaneous frequency

The notion of *instantaneous frequency* of a wave $F(t) = e^{i\phi(t)}$ derives from a stationary phase analysis of the usual Fourier transform integral: we think of the integrand of the Fourier integral

$$f(\omega) = \int F(t)e^{-i\omega t}dt = \int e^{i(\phi(t)-\omega t)}dt \tag{41}$$

as being written in the form $\exp(i\lambda(\phi(t)-\omega t))$, where $\lambda = 1$. The usual large-λ stationary phase calculation shows that the leading order contribution comes from the values of t at which the phase is not changing rapidly with respect to t. This occurs when $0 = (d/dt)(\phi(t) - \omega t)$, or in other words, when $\omega = d\phi/dt$. Thus we call $d\phi/dt$ the *instantaneous frequency* of F.

5.2.2   Chirps

A *chirp* is a finite wavetrain $P(t) = \chi_{\tau/2}(t)\exp(i\phi(t))$ in which the instantaneous frequency changes linearly with time. Here $\chi_{\tau/2}$ denotes the characteristic function of the time interval $[-\tau/2, \tau/2]$, which is one in this time interval

and zero outside. In an *upchirp*, the instantaneous frequency increases linearly with time as $d\phi/dt = \omega_0 + Bt/\tau$, where $\omega_0/2\pi$ is the carrier frequency and $B/2\pi$ is called the *bandwidth*. To determine ϕ, we simply integrate to obtain $\phi(t) = \omega_0 t + Bt^2/(2\tau)$. Thus an upchirp is a wavetrain of the form

$$P(t) = \chi_{\tau/2}(t)e^{i\alpha t^2}e^{i\omega_0 t}, \tag{42}$$

where $\alpha = B/(2\tau)$. We note that such a pulse is of the form (4), where

$$A(t) = \chi_{\tau/2}(t)e^{i\alpha t^2}. \tag{43}$$

5.2.3 Range resolution with chirps

We use (43) in (27) and use the shorthand notation $R_y = |x - y|$, $R_z = |x - z|$:

$$W_R(y, z) = \int \overline{\chi_{\tau/2}(t - 2R_y/c_0)e^{i\alpha(t - 2R_y/c_0)^2}} \chi_{\tau/2}(t - 2R_z/c_0)e^{i\alpha(t - 2R_z/c_0)^2} dt. \tag{44}$$

We expand the squares in the exponentials, and find that the t^2 terms cancel. We are left with

$$W_R(y, z) = e^{i\alpha 4(R_z^2 - R_y^2)/c_0^2} \int_{-\tau/2 + 2\max(R_y, R_z)/2}^{\tau/2 + 2\max(R_y, R_z)/2} e^{i\alpha 4(R_y - R_z)t/c_0} dt \tag{45}$$

The t integral here gives rise to a sinc function of the form

$$\mathrm{sinc}(4\alpha(R_y - R_z)\tau/(2c_0)) = \mathrm{sinc}(B(R_y - R_z)/c_0). \tag{46}$$

The main lobe of this sinc function has a half-width determined by setting the argument equal to π: $B(R_y - R_z)/c_0 = \pi$. This shows that two scatterers can be resolved if their range difference is $R_y - R_z = 2\pi c_0/B$. In other words, better resolution is obtained by using a broad-band wavetrain, as expected.

Many other pulse compression techniques are also possible [8, 5].

6 Acknowledgements

A   Appendix: Technical Details

A.1   Classical scattering theory

To verify (13), we first write $U = \Psi = \Psi^{in} + \Psi^{sc}$ in (1) and use the fact that Ψ^{in} satisfies (13) with $c(x) = c_0$; this give us

$$\left(\nabla^2 - c_0^{-2}\partial_t^2\right)\Psi^{sc} + V\partial_t^2\Psi = 0 \tag{47}$$

We see from applying (3) to (13) that (13) reduces to (47).

We note that (13) shows that the notion of a a point scatterer is problematic. If we take $V(y) = \delta(y - y^0)$ in (13), we obtain

$$\Psi^{sc}(t,z) = \int G_0(t - \tau, z, y^0)\partial_\tau^2\Psi(\tau, y^0)d\tau = \frac{\partial_t^2\Psi(t - |z - y^0|/c_0, y^0)}{4\pi|z - y^0|}, \tag{48}$$

which shows that the scattered field at the point y^0 is singular (unless $\partial_t^2\Psi(t, y^0)$ is zero for all time). But the product of a delta function with a singular function has no conventional meaning. The issue of point scatterers has been studied in [1].

In the Born approximation, however, the field scattered from a point scatterer is well-defined and nonzero.

A.2   Sums of exponentials

$$
\begin{aligned}
\sum_{n=-N/2}^{N/2} e^{ian} &= e^{-iaN/2}\sum_{n=0}^{N}\left(e^{ia}\right)^n \\
&= e^{-iaN/2}\frac{1 - e^{ia(N+1)}}{1 - e^{ia}} \\
&= \frac{e^{ia/2}\left(e^{-ia(N+1)/2} - e^{ia(N+1)/2}\right)}{e^{ia/2}\left(e^{-ia/2} - e^{ia/2}\right)} \\
&= \frac{\sin(a(N+1)/2)}{\sin(a/2)}
\end{aligned}
\tag{49}
$$

A.3   Example: The ERS-1 SAR

The first European Remote sensing Satellite [10], ERS-1, was launched in 1991. Its SAR antenna is a slotted waveguide array, of dimensions $L = 10$m by $D = 1$m. This corresponds to a beamwidth of .288° in azimuth and 5.4° in elevation. The carrier frequency is 5.3GHz, so that $\omega_0 = 2\pi \cdot 5.3 \cdot 10^9$ radians/sec. The system sends out upchirps with bandwidth $B/2\pi$ of 15.5 MHz and a pulse duration τ of 37.1 μs, with a pulse repetition frequency $1/T$ of 1680

Hz. The look angle (i.e., the angle between vertical and the vector normal to the antenna) is 23°. It orbits at an altitude of 785 km and interrogates a 100-km swath whose near and far edges are 200 km and 300 km, respectively, from the projection of the track on the ground.

References

[1] S. Albeverio, F. Gesztesy, R. Høegh-Krohn, and H. Holden, Solvable Models in Quantum Mechanics, Texts and Monographs in Physics, Springer-Verlag, New York, 1988.

[2] M. Cheney, Tomography problems arising in Synthetic Aperture Radar, to appear, Proceedings of the 2000 AMS/IMS/SIAM conference on Radon transforms and tomography.

[3] J.C. Curlander and R.N. McDonough, Synthetic Aperture Radar, Wiley, New York, 1991.

[4] L.J. Cutrona, "Synthetic Aperture Radar", in Radar Handbook, second edition, ed. M. Skolnik, McGraw-Hill, New York, 1990.

[5] H. T. Cuong, A. W. Troesch, T. G. Birdsall, "The Generation of Digital Random Time Histories", Ocean Engineering, 9 (1982) 581–588.

[6] A. Derneryd and A. Lagerstedt, "Novel slotted waveguide antenna with polarimetric capabilities", Proc. of IGARSS Conference, Firenze, Italy (1995) 2054–2056.

[7] A.G. Derneryd, R.N.O. Petersson, P. Ingvarson, "Slotted waveguide antennas for remote sensing satellites", Proceedings of PIERS conferences, Noordwijk, The Netherlands (July 1994).

[8] B. Edde, Radar: Principles, Technology, Applications, Prentice Hall, New York, 1993.

[9] C. Elachi, Spaceborne Radar Remote Sensing: Applications and Techniques, IEEE Press, New York, 1987.

[10] T.-D. Guyenne, ed., Engineering Achievements of ERS-1, European Space Agency SP-1197/III, ESA Publications Division, ESTEC, Noordwij, The Netherlands, 1977.

[11] G. Franceschetti and R. Lanari, Synthetic Aperture Radar Processing, CRC Press, New York, 1999.

[12] K.J. Langenberg, M. Brandfass, K. Mayer, T. Kreutter, A. Brüll, P. Felinger, D. Huo, "Principles of microwave imaging and inverse scattering", EARSeL Advances in Remote Sensing, 2 (1993) 163–186.

[13] K.J. Langenberg, "Applied Inverse Problems", in Basic Methods of Tomography and Inverse Problems, ed. P.C. Sabatier, Adam Hilger, Bristol, 1987.

[14] A.V. Oppenheim and R.W. Shafer, Digital Signal Processing, Prentice-Hall, Englewood Cliffs, New Jersey, 1975.

[15] R.N.O. Petersson, A.G. Derneryd, and P. Ingvarson, "Microstrip antennas for remote sensing satellites", Proceedings of PIERS conferences, Noordwijk, The Netherlands (July 1994).

[16] F. Treves, Basic Linear Partial Differential Equations, Academic Press, New York, 1975.

[17] L.J. Ziomek, Underwater Acoustics: A Linear Systems Theory Approach, Academic Press, Orlando, 1985.

[18] R. Zahn and M. Schlott, "Active antenna for X-band space SAR", Proc. Int. Conf. on Radar, Paris, France, (1994) 36–41.